MEASURING AC MAGNETIC FIELD DISTRIBUTION USING MRI

L. Tugan Muftuler, Y. Ziya Ider
Electrical and Electronics Eng. Dept. Middle East Technical University Ankara TURKEY
e-mail: tugan@rorqual.cc.metu.edu.tr, ideryz@rorqual.cc.metu.edu.tr

Abstract **: Electric currents are applied to body in numerous applications in medicine, such as Electrical Impedance Tomography (EIT), cardiac defibrillators, electrocautery and some treatment methods in physiotherapy. If the magnetic field within a region is measured, the currents generating these fields can be calculated using the curl operator. In this study, magnetic fields generated by AC currents injected into a phantom is measured using MRI. A pulse sequence that is originally designed for mapping static magnetic field is used. AC currents in the form of burst sine wave is applied sychronous with the pulse sequence. Results show that this method can be used in applications where the frequency of the currents is in the audio range and the amplitude is a few milliamperes or larger depending on SNR.**

I. INTRODUCTION

Scott, G.C., et. al., have developed a method to measure the magnetic fields generated by DC currents injected to a sample using MRI [1]. Later, they worked on the measurement of magnetic fields generated by injected RF currents, again using an MRI system [2]. The frequency of applied currents in the second method was the resonance frequency of the MRI system. In both methods, they first measure the magnetic field distribution and then calculate the current density.

However, nobody has yet developed a method to measure the current density in the intermediate frequency range. In this study, a non-invasive method is developed to measure the AC magnetic field generated by AC currents injected into a sample. An MRI system is used for measurements. In this method, the magnetic field component that is parallel to the direction of the main magnetic field of the MRI magnet (z-direction) can be measured. The preliminary studies of this research was reported in [3].

II. MATERIALS AND METHODS

The Pulse Sequence and the Signal Equation:

The MRI pulse sequence used is given in Fig.1. In the absence of an applied AC current, this pulse sequence is the same as the one used by Maudsley A.A. et.al. to calculate the DC magnetic field inhomogeneity [4].

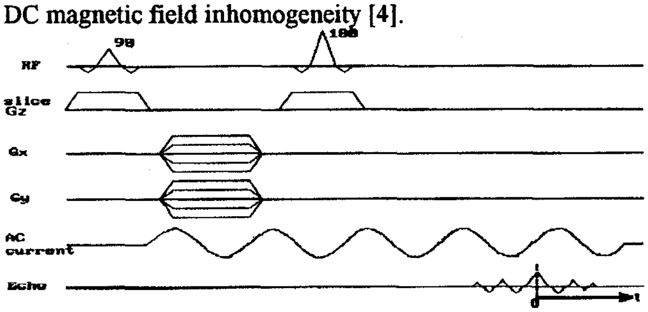

Fig.1. Pulse sequence used for mapping AC magnetic field distribution

During the observation period, if there is no internal AC field distribution, the spins evolve under the influence of the z-component of the static magnetic field inhomogeneity $B(x,y)\cdot \boldsymbol{k}$ only, where $\boldsymbol{k}$ is unit vector in z-direction.

If a time varying magnetic field $b(x,y)\cos(wt)\cdot \boldsymbol{k}$ is added to the static magnetic field inhomogeneity $B(x,y)\cdot \boldsymbol{k}$, then the spin echo signal becomes,

$$s(u,v,t)= \iint m(x,y) e^{i(xu+yv)} e^{i\gamma\int_0^t (B(x,y)+b(x,y)\cos(wt))dt} dxdy$$
$$= \iint m(x,y)\, e^{i(xu+yv)}\, e^{i\gamma(B(x,y)t + b(x,y)\sin(wt)/w)} dxdy \qquad (1)$$

where, $m(x,y)$ is a measure of the density of spins in the transverse slice selected, and γ is a constant. Spatial frequency terms u and v are defined as $u=\gamma*G_x*T_G$ and $v=\gamma*G_y*T_G$, where T_G is the duration of the gradient pulses.

Two dimensional Fourier Transform (2-D FT) with respect to u and v is applied to the acquired data. This operation transforms the data from spatial frequency domain to the space domain. This is depicted in equation (2).

$$S(x,y,t) = F_2\{ s(u,v,t) \} = m(x,y)e^{i\gamma B(x,y)t + i\gamma b(x,y)\sin(wt)/w} \qquad (2)$$

where, F_2 represent 2-D FT operator. By defining $m_f(x,y)= \gamma b(x,y) / w$ and $w_c(x,y)=\gamma B(x,y)$, equation (2) becomes,

$$S(x,y,t) = m(x,y) \cdot e^{i \cdot w_c(x,y)t} \cdot e^{i \cdot m_f \sin(wt)} \qquad (3)$$

$S(x,y,t)$ will be referred to as time variation of voxel value at (x,y). From equation (3), it is seen that the time variation of the voxel value at coordinates (x,y) is the same as that of a single-tone wide band FM signal [5].

We take the natural logarithm of both sides of (3),

$$\ln(S(x,y,t)) = \ln(m(x,y)) + i\cdot w_c(x,y)\cdot t + i\cdot\phi_1 + i\cdot m_f \sin(wt+\phi_2) \qquad (4)$$

where, ϕ_1 is the phase of the echo signal and ϕ_2 is the phase of the injected current at t=0. The imaginary part of equation (4) defines a new temporal signal for each voxel at coordinates (x,y). We call this function $f(x,y,t)$,

$$\begin{aligned} f(x,y,t) &= w_c(x,y)\cdot t + \phi_1 + m_f(x,y)\cdot\sin(wt+\phi_2) \\ &= w_c(x,y)\cdot t + \phi_1 + m_f(x,y)\cdot\cos(\phi_2)\cdot\sin(wt) \\ &\quad + m_f(x,y)\cdot\sin(\phi_2)\cdot\cos(wt) \end{aligned} \qquad (5)$$

from which we form a set of linear equations,

$$\mathbf{f} = \mathbf{A} \cdot \mathbf{x} \qquad (6)$$

where $\mathbf{f}=[f(x,y,t_0),\ldots, f(x,y,t_M)]^T$ is our measurement vector, coefficient matrix $\mathbf{A}$ contains known parameters and

0-7803-3811-1/97/$10.00 ©IEEE

$x=[w_c(x,y)\ \phi_1\ m_f(x,y)\cos(\phi 2)\ m_f(x,y)\sin(\phi 2)]^T$ is the vector of unknowns. From the overdetermined system of equations (6), x is computed in the least square sense,

$$A^T \cdot f = A^T \cdot A \cdot x \Rightarrow (A^T \cdot A)^{-1} \cdot A^T \cdot f = x \quad (7)$$

We calculate the AC field,

$$\phi_2 = \arctan(x(4)/x(3))$$

$$\Rightarrow m_f(x,y)=(x(3)/\cos(\phi 2) \Rightarrow b(x,y) = mf(x,y)\,(w/\gamma) \quad (8)$$

Experiments

In our experiments, a 0.15 T MRI system, designed and developed in our laboratory, is used [6]. FOV is 24cm*24cm with 32 samples in each direction and 128 samples are acquired from each echo. Sampling frequency is 4KHz and slice thickness is 1.3cm with TE=39ms, TR=600ms. A plexiglass phantom filled with $CuSO_4$ doped saline solution with inner dimensions 13mm*95mm*95mm is used (Fig.2.) Current is injected through three plastic tubes each 50mm

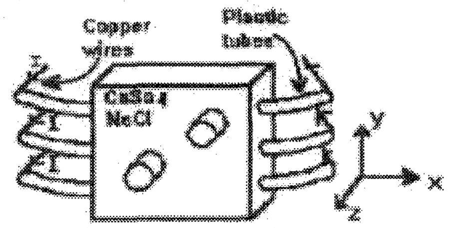

Fig.2. The phantom used (not drawn to scale)

long and sunk by another set of three tubes on the opposite side. Two plastic cylinders with 15mm diameter and 13mm height is prepared to simulate the conductivity change. They are filled with the same solution. Injected AC current is synchronised with the pulse sequence. Duration of each sinusoidal burst current is 200ms.

Two basic studies are conducted. In the first study two different magnetic field map data are acquired. The first set of data is acquired from the square phantom with no cylinders, whereas the second is acquired with the cylinders placed diagonally within the square phantom. The amplitude of the injected current is 154ma (rms) and the frequency is 100Hz. Four-fold signal averaging is used to increase SNR. Second study is carried out to determine the minimum useable current amplitude and frequency. Frequency of the current is kept at 100Hz while the amplitude is decreased. In this study eight-fold signal averaging is used.

III. Results and Discussion

The difference of the two fields acquired at 154ma is plotted in Fig.3. It can be seen that a conductivity change within the object to be imaged results in perturbations in AC field distribution around regions where conductivity changes.

When the injected current is 15ma (rms) and the frequency is 100Hz, the peaks due to the conductivity change become comparable with the noise peaks in the AC magnetic field image. However, if larger insulating objects are placed in the square phantom, keeping current amplitude and frequency constant, SNR of the magnetic field image increases; whereas, the SNR of the image decreases if the

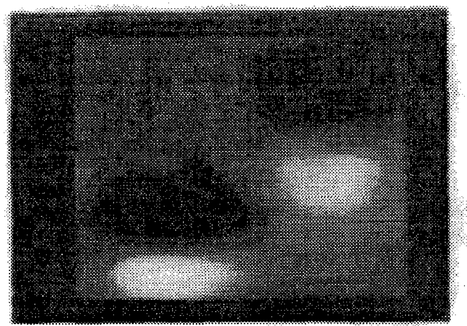

Fig. 3. Difference of AC magnetic field in a phantom of homogenous conductivity and AC magnetic field in the same phantom with two circular insulator objects in it. (the phantom is described in Fig. 2.)

magnitude of conductivity perturbations gets smaller. The frequency of the applied current is in the audio range but is not fixed. However, the SNR decreases with increasing frequency.

The noise figure of our receiver system is approximately 3dB. It is stated that the signal strength is directly proportional to the applied main magnetic field strength [7]. Therefore, with a higher field strength and with a low noise preamplifier, the magnetic fields generated by the currents in medical Electrical Impedance Tomography (EIT) applications can be calculated using MRI. In [8] it is expressed that currents up to 5mA (rms) can be injected to human body without any risk as far as there is no catheter inserted near the heart region. Once the magnetic field distribution is measured (at least in three directions), one can calculate the currents generating these magnetic fields. In theory, any information regarding the internal current distribution can be incorporated into the EIT reconstruction algorithms in order to increase spatial resolution.

In our experiments, sinusoidal currents are applied. However, any current with a known pulse shape can be applied as long as it is synchronised with the pulse sequence. Resulting magnetic fields can be calculated with the proposed algorithm.

IV. References

[1] G.C.Scott, M.L.G. Roy, R.L. Armstrong, R.M. Henkelman:"Measurement of Nonuniform Current Density by Magnetic Resonance", IEEE Tr. Med. Img., v. 10, iss. 3, pp 362-374, 1991.

[2] G.C.Scott, et.al. "Electromagnetic Considerations for RF Current Density Imaging", IEEE Tr. Med. Img., v. 14, iss. 3, pp 515-524, 1995.

[3] Y.Z.Ider, L.T.Muftuler, "Use of MRI for Measuring AC Internal Currents of EIT: a Feasibility Study", 9th Int. Conf. Electrical Bioimpedance in conj. with European Community Concerted Action on Impedance Tomography, pp 420-421, Sept. 26-30 1995.

[4] A.A. Maudsley, H.E. Simon, S.K. Hilal, "Magnetic Field Measurement by NMR Imaging" J. Phys. E: Sci. Instr., v. 17, pp 216-220,1984.

[5] S. Haykin, Communication Systems, John Wiley & Sons, pp 180-219, second edition, 1983.

[6] L.T. Muftuler, et.al. "Low Cost PC Based Whole Body Magnetic Resonance Imaging System", 15th Int. Ann. Mtg. of IEEE EMBS, pp 184-185, Oct. 28-31,1993. San Diego USA

[7] P.G. Morris, "Nuclear Magnetic Resonance Imaging in Medicine and Biology", Clarendon Press Oxford, pp 12-27, 1986.

[8] R. Aston, "Principles of Biomedical Instrumentation and Measurement", Merrill Publishing Comp., USA pp 49-56, 1990.